JACS
JOURNAL OF THE AMERICAN CHEMICAL SOCIETY
Article
pubs.acs.org/JACS

Reversible Generation of a Carbon-Centered Radical from Alkyl Iodide Using Organic Salts and Their Application as Organic Catalysts in Living Radical Polymerization

Atsushi Goto,* Akimichi Ohtsuki, Haruki Ohfuji, Miho Tanishima, and Hironori Kaji*

Institute for Chemical Research, Kyoto University, Uji, Kyoto 611-0011, Japan

Supporting Information

ABSTRACT: A new method of producing carbon-centered radicals was discovered through the reaction of an alkyl iodide (R-I) with organic salts to reversibly generate the corresponding alkyl radical ($R^{\bullet}$). Via this new reaction, the organic salts were used as new and highly efficient organic catalysts in living radical polymerization. The catalysts included common and inexpensive compounds such as tetrabutylammonium iodide and methyltributylphosphonium iodide. Notably, the catalysts were highly reactive. They enabled the synthesis of high-molecular-weight polymers (up to M_n = 140 000) and the control of acrylate polymerization, which had been difficult with other organic catalysts. The organic salt catalysts were highly versatile, reacting with methacrylate, acrylate, styrene, acrylonitrile, and functional methacrylate monomers. Well-defined block copolymers were also prepared by using this method. A kinetic study quantitatively confirmed the high reactivity of these catalysts. Attractive features of this system include its low cost, its ease of operation, and its ability to access a wide range of polymer designs.

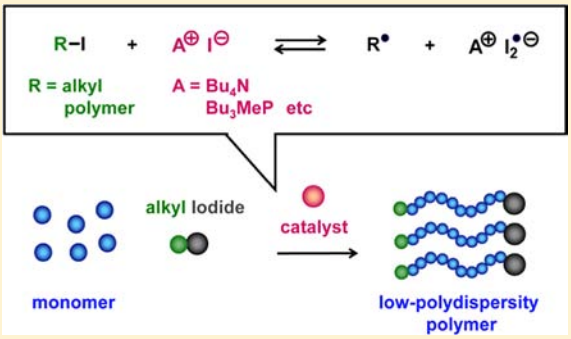

INTRODUCTION

Organic catalysts have been extensively studied for decades. Many of these catalysts are environmentally benign, inexpensive, easily handled, and thus offer attractive synthetic approaches in organic chemistry. The recent development of organic catalysts for fine reactions has particularly drawn attention to organic catalysts.[1]

Our group is interested in the reversible generation of a carbon-centered radical ($R^{\bullet}$) from an alkyl iodide (R-I) via organic catalysis. We have applied this fundamental reaction in living radical polymerization (LRP) to synthesize well-defined polymers. In our previous work, we investigated two reaction types. The first reaction type was the chain transfer reaction of R-I with organic radical catalysts to reversibly generate $R^{\bullet}$. Inspired by the well-known "irreversible" reactions of R-I with tin and germanium radicals to generate $R^{\bullet}$,[2] we recently developed the corresponding reversible reactions by carefully choosing the radical catalysts (germanium, phosphorus, nitrogen, oxygen, and carbon-centered radical catalysts). We then developed a new LRP that we termed reversible chain transfer catalyzed polymerization (RTCP).[3−6] The second reaction type was the reaction of R-I with amine catalysts to reversibly generate $R^{\bullet}$. Again inspired by relevant "irreversible" reactions in organic chemistry,[7] we developed the reversible reactions by exploiting appropriate amine catalysts, and we subsequently developed a new LRP that we termed reversible complexation mediated polymerization (RCMP).[6,8−10]

LRP has gained substantial attention in polymer chemistry because it allows for the rational design of polymer architectures with predictable molecular weights and narrow molecular weight distributions.[11−15] Mechanistically, LRP is based on the reversible activation of a dormant species (Polymer-X) to a propagating carbon-centered radical (Polymer$^{\bullet}$) (Scheme 1a). A sufficiently large number of activation−deactivation cycles are required for achieving low polydispersity.[16] Examples of the capping agent (X) are nitroxides, dithioesters, tellurides, and halogens.[12−14] The halogen capping

Scheme 1. Reversible Activation: (a) General Scheme, (b) ATRP, and (c) RCMP

(a) Reversible activation (general scheme)

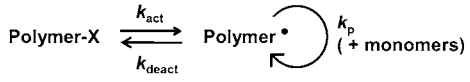

(b) ATRP (Ru, Cu, etc for transition metal)

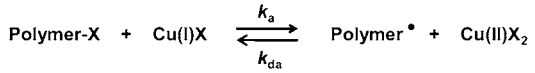

(c) RCMP

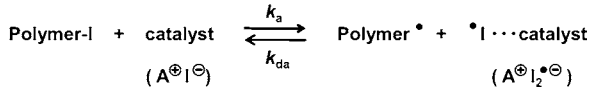

Received: April 11, 2013
Published: July 19, 2013

   dx.doi.org/10.1021/ja4036016 | J. Am. Chem. Soc. 2013, 135, 11131−11139

agents are combined with transition metal catalysts to induce the reversible activation, and this metal-catalyzed system is called atom transfer radical polymerization (ATRP) (Scheme 1b).[13]

RTCP and RCMP use iodine as X. They were the first LRPs to use organic catalysts for the reversible activation. A prominent feature of these systems is that no special capping agents or metals are used. The catalysts are inexpensive, relatively nontoxic, easy to handle, and also amenable to a variety of functional groups and monomers. These systems are facile and pervasive methodologies that may find some practical use. However, both RTCP and RCMP have important limitations, particularly with respect to monomer versatility and molecular weight. The monomer scope was limited to styrenics and methacrylates, and the controlled polymerization of acrylates was unattainable. The molecular weight was limited to approximately 10 000 in most cases. Higher molecular weights are important in material design for tuning mechanical, thermodynamic, and optical properties.

To address these challenges, we pursued more reactive catalysts. For RCMP (Scheme 1c), we developed a unique reaction of R-I with iodide anions (as catalysts) to reversibly generate R•. The use of iodide in this manner is unprecedented in chemistry. In the described experiments, we employed organic salts such as quaternary ammonium and phosphonium iodides (Figure 1). An encouraging feature of these organic salts was their high reactivity.

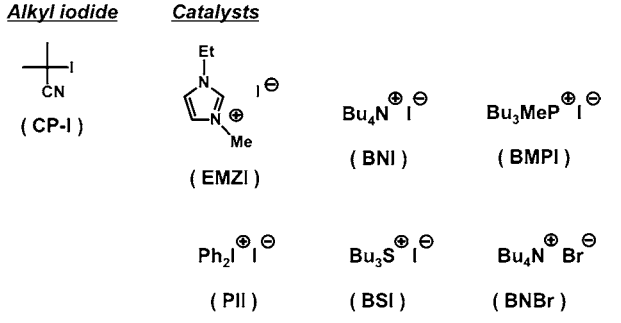

Figure 1. Structures of CP-I and catalysts used in this work.

In this paper, we report this unique reaction of organic salts and their application as powerful and pervasive catalysts for RCMP. Examples of the catalysts employed are $Bu_3MeP^+I^-$ (BMPI), $Bu_4N^+I^-$ (BNI), and ethylmethyl imidazolium iodide (EMZI) (Figure 1). These catalysts are among the most inexpensive organic salts and may be suitable for practical use. These organic salts also exhibited high catalytic activity. Notably, they allowed for the synthesis of high-molecular-weight methacrylate polymers and the control of acrylate polymerization, which had been difficult with our previous organic catalysts. The organic salt catalysts in this paper had a monomer scope that encompassed all of the three important monomers for radical polymerization (methacrylates, acrylates, and styrene (St)) and also acrylonitrile (AN) and functional monomers. The catalysts also afforded block copolymers. Ease of use and access to a wide range of polymer designs are two highly desirable features of this polymerization technique.

RESULTS AND DISCUSSION

Experimental Proof of Generation of R• from R-I with Organic Salts. A radical trap experiment[10,17] was performed to show the generation of R• from R-I with organic salts. We used 2-cyanopropyl iodide (CP-I) (Figure 1) as the R-I. We studied iodide (I^-) salts in the form of EMZI (imidazolium salt), BNI (ammonium salt), BMPI (phosphonium salt), $Ph_2I^+I^-$ (PII) (iodinium salt), and $Bu_3S^+I^-$ (BSI) (sulfonium salt) (Figure 1). In addition, we studied a bromide (Br^-) salt in the form of $Bu_4N^+Br^-$ (BNBr) (ammonium salt) (Figure 1). In each radical trap trial, we heated CP-I (10 mM), an organic salt (80 mM), and the radical trap 2,2,6,6-tetramethylpiperidinyl-1-oxy (TEMPO) (20 mM) at 60 °C in a mixture of toluene-d_8 and acetonitrile-d_3 (9:1). If CP-I reacts with the organic salt, the generated radical CP• is trapped by TEMPO, thereby yielding CP-TEMPO. Figure 2 shows the ^{1}H NMR spectra at time zero

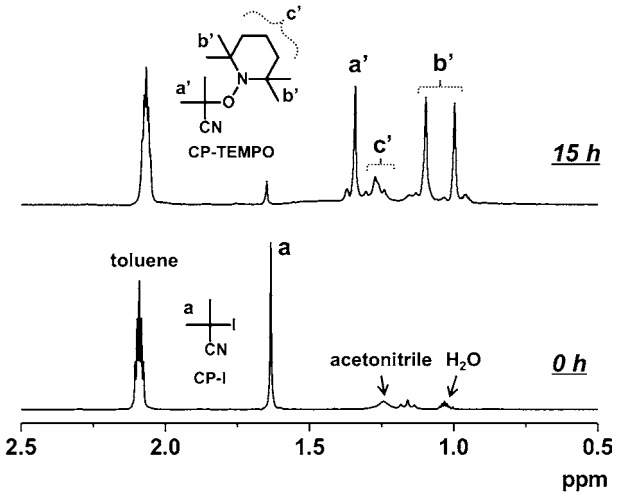

Figure 2. ^{1}H NMR spectra (in the range of 0.5−2.5 ppm) of the solution of CP-I (10 mM), EMZI (80 mM), and TEMPO (20 mM) heated at 60 °C for 0 and 15 h. The solvent was a mixture of toluene-d_8 and acetonitrile-d_3 (9:1).

and at 15 h for EMZI. At 15 h, new signals appeared and matched those of pure CP-TEMPO that was independently prepared (Supporting Information). The extent of reaction of CP-I to CP-TEMPO was 88%. The result clearly demonstrates the generation of R• from R-I with an organic salt.

Table 1 lists the extent of reaction of CP-I for the six studied organic salts. The reaction occurred in all cases. Among the

Table 1. Extent of Reaction of CP-I with Organic Salts

entry	organic salt	reaction extent (%)[a]
1	EMZI	88
2	BNI	74
3	BMPI	73
4	PII	73
5	BSI	27
6	BNBr	55

[a]The extent of reaction of CP-I to CP-TEMPO via the reaction of CP-I (10 mM), an organic salt (80 mM), and TEMPO (20 mM) at 60 °C for 15 h. The solvent was a mixture of toluene-d_8 and acetonitrile-d_3 (9:1).

iodide salts, BNI, BMPI, and PII were as effective as EMZI (entries 1−4). BSI was less effective than the other four salts (entry 5). The bromide salt BNBr worked as well (entry 6), although the corresponding iodide BNI was more reactive. These results indicate that a wide range of cations and anions

dx.doi.org/10.1021/ja4036016 | J. Am. Chem. Soc. 2013, 135, 11131−11139

can be used in this reaction and that the reactivity depends on the selected cations and anions. In the absence of TEMPO, the reaction was reversible. Taking advantage of this reversible nature, we utilized the organic salts as catalysts for RCMP, as described in subsequent sections.

Polymerizations of MMA with Three Different Catalysts. We used EMZI, BNI, and BMPI as catalysts in the RCMPs of methyl methacrylate (MMA). EMZI, BNI, and BMPI were selected because of their inexpensiveness and observed high reactivity (Table 1). We heated a mixture of MMA (8 M), CP-I (80 mM) as a low-mass dormant species, and a catalyst (40 mM) at 70 °C (Figure 3 and Table 2 (entries 1−3)). In this system (Scheme 1c), the organic salt (A^+I^-) works as an activator of Polymer-I to produce Polymer$^\bullet$ and $A^+I_2^{\bullet-}$. A few monomers are incorporated into Polymer$^\bullet$ until Polymer$^\bullet$ is deactivated by $A^+I_2^{\bullet-}$ to give Polymer-I and A^+I^- again. As the activation−deactivation cycles are repeated, the polymer chain grows little by little, yielding a low-polydispersity polymer.

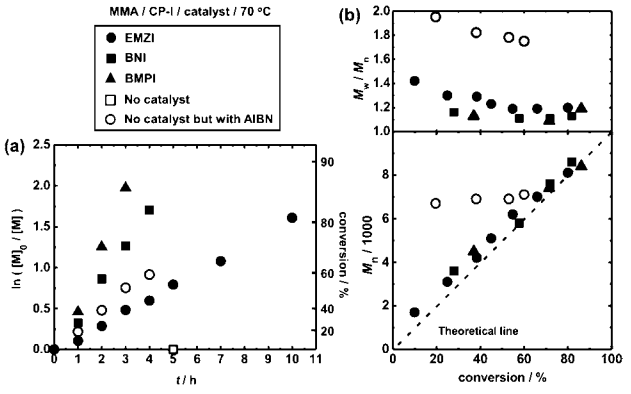

Figure 3. Plots of (a) $\ln([M]_0/[M])$ vs t and (b) M_n and M_w/M_n vs conversion for the MMA/CP-I/catalyst systems (in bulk) (70 °C): $[MMA]_0$ = 8 M; $[CP\text{-}I]_0$ = 80 mM; $[catalyst]_0$ = 40 mM (EMZI, BNI, and BMPI) or $[AIBN]_0$ = 10 mM (no catalyst but with AIBN). The symbols are indicated in the figure.

As Figure 3a (filled symbols) shows, the polymerization proceeded to about 80% monomer conversion in 3−10 h for each of the three catalysts. In all cases, the first-order plot of the monomer concentration ([M]) was linear in the studied range of time (t). No polymerization occurred in the absence of a catalyst (Figure 3a (open square)). These results mean that the radical was generated because of the reaction of CP-I (and Polymer-I) with the catalyst. In the studied cases, because the $[MMA]_0/[CP\text{-}I]_0$ ratio was set to 100, the degree of polymerization (DP) expected at full (100%) monomer conversion was 100. Figure 3b (filled symbols) shows that the number-average molecular weight (M_n) linearly increased as the conversion increased and agreed well with the theoretical value ($M_{n,theo}$). The polydispersity index (PDI = M_w/M_n, where M_w is the weight-average molecular weight) was about 1.2 from an early stage of polymerization, which indicates a high frequency of the activation−deactivation cycle. Importantly, PDI also remained small (about 1.2) through high conversions (about 80%), thereby illustrating the usefulness of RCMP.

Mechanistically, not only reversible complexation (RC) (Scheme 1c) but also degenerative chain transfer (DT) (activation of Polymer-I by Polymer$^\bullet$)[14,16] occurs as an activation process. However, the contribution of DT is minor. Figure 3 (open circles) shows the pure DT system (iodide-mediated polymerization), which did not include a catalyst (RC) but did include azobis(isobutyronitrile) (AIBN) as a radical initiator (DT). Only large PDI values (>1.7) were observed with this pure DT system, which clearly indicates that the regulated polydispersity in RCMP arises primarily from the work of the catalyst (RC) with only a small contribution from DT.

Among the three catalysts, the smallest PDI was achieved with BNI, which suggests that its activation rate constant k_a (frequency of the activation−deactivation cycle) is the largest (Scheme 1c). The kinetic study presented below verified that inference. The largest polymerization rate R_p (and hence [Polymer$^\bullet$]) was observed with BMPI. This fact suggests that the equilibrium constant K (= k_a/k_{da} in Scheme 1c) is the largest with BMPI.

Notably, the three catalysts exhibited high reactivity. Figure 4 compares the results of BMPI and triethylamine (TEA),[8] which is a previously studied amine catalyst. BMPI at 80 °C (filled circles) afforded a larger R_p and lower polydispersity than TEA at 90 °C (open circles), demonstrating the higher reactivity of BMPI even at lower temperatures. BMPI at 70 °C (squares) and TEA at 90 °C led to similar polymerization rates. BMPI at 60 °C (triangles) still afforded a sufficiently large R_p, and a high conversion (80%) was reached in a fairly short time (8 h). We

Table 2. Polymerizations of MMA

entry	target DP	catalyst	$[MMA]_0/[CP\text{-}I]_0/[catalyst]_0$ (mM)	additive	solvent	T (°C)	t (h)	conv (%)	M_n ($M_{n,theo}$)	PDI
1	100	EMZI	8000/80/40	-	bulk	70	10	80	8100 (8000)	1.20
2	100	BNI	8000/80/40	-	bulk	70	4	82	8600 (8200)	1.13
3	100	BMPI	8000/80/40	-	bulk	70	3	86	8400 (8600)	1.19
4	100	BMPI	8000/80/40	-	bulk	80	2	83	8300 (8300)	1.26
5	100	BMPI	8000/80/40	-	bulk	60	8	78	7700 (7800)	1.14
6	400	BMPI	8000/20/80	-	bulk	60	12	71	30000 (28000)	1.19
7	800	BMPI	8000/10/80	-	toluene[a]	60	48	72	56000 (58000)	1.29
8	800	BMPI	8000/10/80	PMDETA[b]	toluene[a]	60	24	94	83000 (75000)	1.35
9	800	BMPI	8000/10/80	V70[c]	toluene[a]	40	17	96	73000 (77000)	1.31
10	800	BNI	8000/10/80	V70[c]	toluene[a]	40	24	99	70000 (79000)	1.32
11	1600	BMPI	8000/5/80	-	toluene[a]	60	48	60	83000 (96000)	1.37
12	1600	BMPI/BNI	8000/5/(80/80)	PMDETA[b]	toluene[a]	60	24	93	140000 (150000)	1.36

[a]Diluted in 25 wt % toluene (solution polymerization). [b]$[PMDETA]_0$ = 20 mM (entry 8) and 80 mM (entry 12). [c]$[V70]_0$ = 5 mM (entries 9 and 10).

dx.doi.org/10.1021/ja4036016 | J. Am. Chem. Soc. 2013, 135, 11131−11139

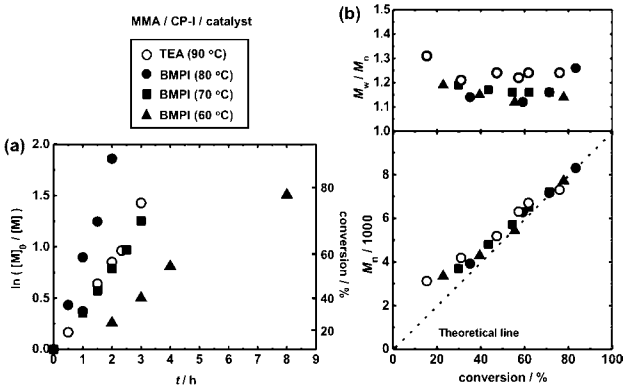

Figure 4. Plots of (a) $\ln([M]_0/[M])$ vs t and (b) M_n and M_w/M_n vs conversion for the MMA/CP-I/catalyst systems (in bulk): $[MMA]_0$ = 8 M; $[CP\text{-}I]_0$ = 80 mM; $[catalyst]_0$ = 40 mM. The catalysts, temperatures, and symbols are indicated in the figure.

took advantage of such high reactivity in the subsequently described studies.

Chain End Fidelity. To examine the livingness (chain end fidelity) in this polymerization, we carried out elemental analysis and NMR analysis of the polymers obtained with BMPI at 60 °C in Figure 4 (filled triangles).

The polymers obtained for 2, 4, and 8 h in Figure 4 (filled triangles) were purified by preparative GPC to remove a trace of impurities such as a residual BMPI catalyst. The M_n and PDI before and after the purification are listed in Table 3. The M_n and PDI were determined by GPC calibrated with standard poly(methyl methacrylates)s (PMMAs).

Table 3. Elemental Analysis of Polymers Obtained in Figure 4 (Filled Triangles)

time	purification	M_n	PDI	I(exp) (%)	I(theo) (%)	fraction of iodide chain end (%)
2 h	before	3300	1.19			
	after	3400	1.19	3.72	3.74	99
4 h	before	5400	1.12			
	after	5600	1.12	2.08	2.27	92
8 h	before	7700	1.14			
	after	8100	1.13	1.44	1.57	92

Table 3 shows the results of the elemental analysis for the three polymers after the purification. I(exp) is the iodine content experimentally determined by elemental analysis. I(theo) is the iodine content theoretically calculated from the M_n determined by GPC and on the assumption that all of the polymer chains possess iodine at the chain end. The fraction of iodine chain end was calculated by I(exp)/I(theo). The elemental analysis of iodine showed that the polymers obtained at 2 h (23% conversion), 4 h (56% conversion), and 8 h (78% conversion) included high fractions, i.e., 99%, 92%, and 92%, of active polymer possessing iodine at the chain end, respectively (with ±5% experimental error).

The polymer for 2 h after purification was subjected to high-resolution 800 MHz ^{1}H NMR measurement (Figure 5). (For the higher molecular weight polymers at 4 and 8 h, quantitative analysis of the polymer chain end by NMR was difficult.) The methyl protons (a, a′, and a″) at the side chain appered at 3.55−3.76 ppm. The main peak at 3.55−3.63 ppm and its side peak at 3.63−3.65 ppm are assigned to the monomer units (a) in the middle of the chain. (The side peak at 3.63−3.65 ppm

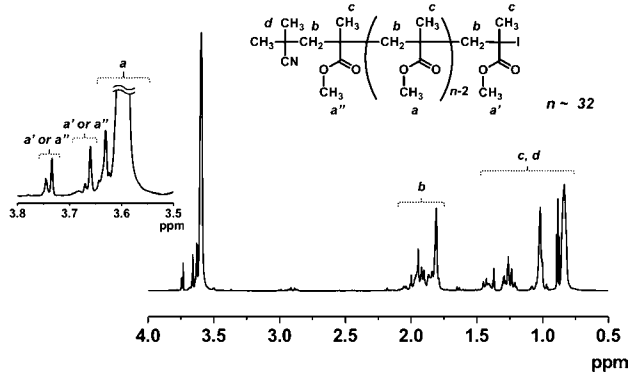

Figure 5. Plots of ^{1}H NMR spectrum (in the range of 0.5−4.0 ppm) of the polymer for 2 h after purification in Table 3 (in $CDCl_3$).

may be due to a chain-end penulutimate unit.) A downfield-shifted peak at 3.73−3.76 ppm would be assigned to the ω-terminal chain-end unit (a′) adjacent to iodine. Such a downfield shift for the ω-terminal chain-end unit was reported for PMMA-bromide.[18] From the peak area and the M_n deteremined by GPC, the fraction of the iodine chain end was calculated to be 97%. A peak at 3.65−3.69 ppm would be due to the α-terminal chain-end unit (a″) adjacent to the 2-cyanopropyl (CP) group. However, the assignment is not definitive, and the peak at 3.65−3.69 ppm can be due to the ω-terminal chain-end unit (a′). In this case, the fraction of iodine chain end was calculated to be 99%. The elemental analysis and NMR analysis demonstrate good livingness (high chain end fidelity) in this polymerization.

Toward High Molecular Weights. The polymer produced in RCMP contains iodine at the chain end. For methacrylate polymers, decomposition (elimination of HI (Scheme 2))

Scheme 2. Decomposition of Polymer-I (Elimination of HI from Polymer-I) for Methacrylate Polymer

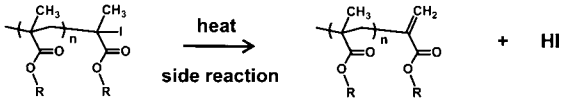

occurs upon heating to produce a dead chain. A mild temperature such as 60 °C can suppress this side reaction and might enable the synthesis of high-molecular-weight polymers. Thus, we used 60 °C for the MMA polymerization and targeted 400, 800, and 1600 DPs at 100% conversion. We chose BMPI as a catalyst to maintain a sufficiently large R_p at the mild polymerization temperature. Figure 6 and Table 2 (entries 6, 7, and 11) show the results. Toluene was used as a solvent for the targeted DPs of 800 and 1600 to decrease the viscosity of the solution. In all cases, we obtained low-polydispersity (PDI = 1.1−1.4) polymers up to high conversions, i.e., polymers with molecular weights of up to several tens of thousands.

For the targeted DPs of 800 and 1600, the polymerization was rather slow (i.e., it required 2 days) because of the low concentration of CP-I. In these systems, the slow polymerization was overcome with the addition of an amine or a small amount of an azo compound (Figure 7 and Table 2). An amine traps the radical polymerization inhibitor HI (Scheme 2) and also functions as an additional activator to increase R_p. An azo compound supplies Polymer$^\bullet$ to increase R_p. Azo compounds

dx.doi.org/10.1021/ja4036016 | J. Am. Chem. Soc. 2013, 135, 11131−11139

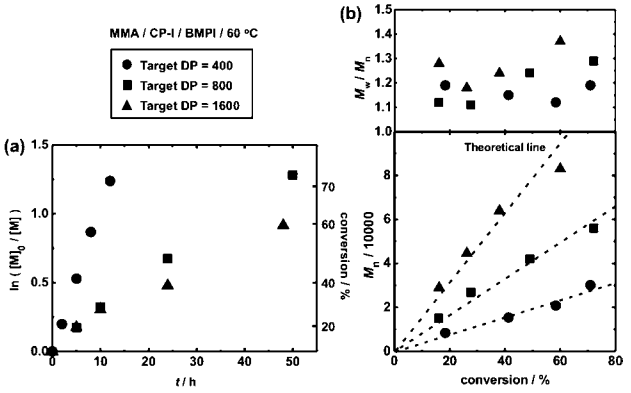

Figure 6. Plots of (a) $\ln([M]_0/[M])$ vs t and (b) M_n and M_w/M_n vs conversion for the MMA/CP-I/BMPI systems (60 °C): $[MMA]_0$ = 8 M; $[CP\text{-}I]_0$ = 20, 10, and 5 mM for the targeted DPs = 400, 800, and 1600, respectively; $[BMPI]_0$ = 80 mM. The polymerization was in bulk (targeted DP = 400) or in 25 wt % toluene (targeted DP = 800 and 1600). The symbols are indicated in the figure.

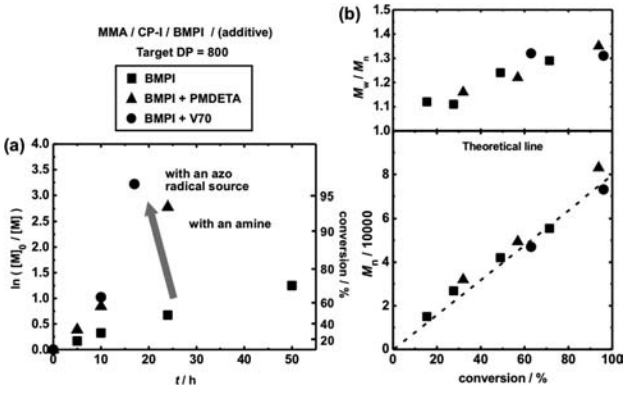

Figure 7. Plots of (a) $\ln([M]_0/[M])$ vs t and (b) M_n and M_w/M_n vs conversion for the MMA/CP-I/BMPI/(additive) systems (in 25 wt % toluene): $[MMA]_0$ = 8 M; $[CP\text{-}I]_0$ = 10 mM; $[BMPI]_0$ = 80 mM. The additives were PMDETA (20 mM) and V70 (5 mM). The temperature was 60 °C (no additive and PMDETA) or 40 °C (V70). The symbols are indicated in the figure.

have often been used to increase R_p in other LRP systems.[16] Figure 7 and Table 2 (entries 7−9) show the results for the targeted DP of 800. The R_p dramatically increased by a factor of about four with the addition of pentamethyldiethylenetriamine (PMDETA) at 60 °C. The R_p further increased by a factor of about seven with the addition of 2,2′-azobis(4-methoxy-2,4-dimethyl valeronitrile) (V70) at an even lower temperature of 40 °C. Moreover, the additives did not significantly affect M_n or PDI, whereas their addition greatly increased R_p. The amine was also utilized for the targeted DP of 1600, yielding a 140 000 molecular weight polymer with a PDI of 1.36 in 24 h (Table 2 (entry 12)). V70 accelerated R_p for BNI as well (Table 2 (entry 10)). Thus, low-polydispersity polymers were obtained in the 10^4−10^5 molecular weight range within reasonable times.

Polymerization of Acrylate. The carbon−iodine bond in an acrylate polymer (with a secondary alkyl chain end) is stronger than that in the methacrylate polymer (with a tertiary one). The greater strength of this bond indicates that highly reactive catalysts are required for controlling acrylate polymerization. BMPI and BNI were thus used for butyl acrylate (BA) polymerization. Figure 8 and Table 4 show the results with BA (8 M), CP-I (80 mM), and each catalyst (320 mM) at 110 °C.

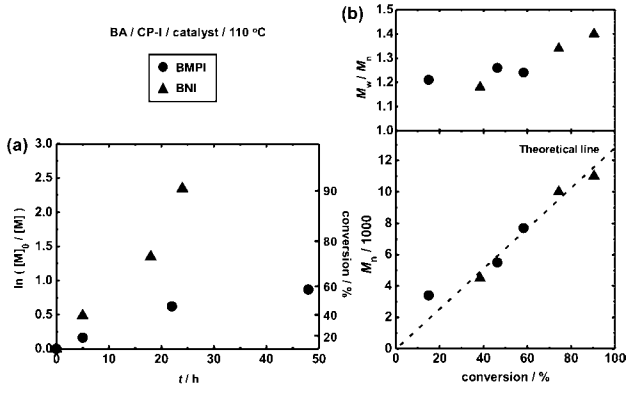

Figure 8. Plots of (a) $\ln([M]_0/[M])$ vs t and (b) M_n and M_w/M_n vs conversion for the BA/CP-I/catalyst systems (in bulk) (110 °C): $[BA]_0$ = 8 M; $[CP\text{-}I]_0$ = 80 mM; $[catalyst]_0$ = 320 mM. The catalysts and symbols are indicated in the figure.

Because of the high reactivity, the polymerization exhibited characteristics of a living process and yielded low-polydispersity polymers (PDI = 1.2−1.4) for both catalysts. For BA, BNI afforded a larger R_p than did BMPI, in contrast to MMA (Figure 3). A high conversion (90%) was reached for 24 h with BNI. These results illustrate successful acrylate polymerizations.

Block Copolymerizations of Methacrylates and Acrylate. Exploiting the living character of our system, we performed block copolymerizations (Table 5). Starting from a purified PMMA macroinitiator (PMMA-I) (M_n = 5500 and PDI = 1.15), polymerizations of glycidyl methacrylate (GMA) and BA yielded the well-defined methacrylate/methacrylate and methacrylate/acrylate block copolymers (entries 1 and 2). Figure 9 shows the full distribution molecular weight distributions (GPC chromatograms). A large faction of the macroinitiator chains was extended to block copolymers. This clearly confirms high block efficiency, due to the high chain end fidelity as demonstrated above.

Markedly, for the MMA/BA system, even a poly(butyl acrylate) macroinitiator (PBA-I) (M_n = 10 000 and PDI = 1.33) afforded a well-defined copolymer (entry 3). In some LRP systems, the synthetic order of the two blocks is crucial when two different families of monomer are used.[11,19] Thus, the lack of restriction in the synthetic order of the two blocks in the present system is interesting.

Instead of the use of an isolated macroinitiator (entries 1−3), successive addition of two monomers was also performed (entries 4 and 5). When a low-mass CP-I was used as a starting material, methacrylate/acrylate (MMA/BA) block copolymers with small PDIs were obtained, again without the restriction of the monomer order of addition. Figure 9 also confirms high block efficiency. These examples demonstrate our system's high accessibility to a variety of block copolymers.

Use of Alkyl Iodide Formed In Situ. In the previously described studies, we employed a preformed R-I (e.g., CP-I) as the starting dormant species. Instead of a preformed R-I, molecular iodine (I_2) and an azo compound (R−N=N−R) can be used as starting compounds; then, for the polymerization, the R-I formed in situ can be used. We previously showed that this (I_2/azo) method is effective for RTCP[4,6] and RCMP.[9] The method was originally invented by Lacroix-Desmazes et al.[14,20] for iodide-mediated LRP and may be practically useful because of the general long-term instability of

dx.doi.org/10.1021/ja4036016 | J. Am. Chem. Soc. 2013, 135, 11131−11139

Table 4. Polymerizations of BA

entry	target DP	catalyst	$[BA]_0/[CP\text{-}I]_0/[catalyst]_0$ (mM)	solvent	T (°C)	t (h)	conv (%)	M_n[a] ($M_{n,theo}$)	PDI[a]
1	100	BNI	8000/80/320	bulk	110	24	90	11000 (11000)	1.39
2	100	BMPI	8000/80/320	bulk	110	48	58	7700 (7400)	1.24

[a]Determined by gel permeation chromatography (GPC) with a multiangle laser light-scattering (MALLS) detector.

Table 5. Block Copolymerizations

entry	monomer	target DP	catalyst	alkyl iodide	$[monomer]_0/[alkyl\ iodide]_0/[catalyst]_0$ (mM)	solvent	T (°C)	t (h)	conv (%)	M_n[a] ($M_{n,theo}$)	PDI[a]
1	GMA	200	BMPI	PMMA-I[b]	8000/40/80	bulk	60	6	71	24000 (25000)	1.23
2	BA	100	BNI	PMMA-I[b]	8000/80/320	bulk	110	24	65	15000 (16000)	1.31
3	MMA	100	BNI	PBA-I[c]	8000/80/320[d]	bulk	110	5	86	16000 (20000)	1.31
4	MMA	100	BMPI	CP-I	8000/80/80	bulk	60	5	83	8400 (8300)	1.10
	+BA	+100	BNI		8000/0/320	bulk	110	24	155	18000 (18000)	1.32
5	BA	100	BNI	CP-I	8000/80/320	bulk	110	22	82	13000 (11000)	1.28
	+MMA	+100			8000/0/0[d]	toluene[e]	110	5	170	27000 (21000)	1.39

[a]Determined by GPC with a MALLS detector for the first block in entry 5 and PMMA-calibration for the others. [b]PMMA-I (M_n = 5100 and PDI = 1.15). [c]PBA-I (M_n = 10 000 and PDI = 1.33). [d]With the addition of I_2 (4 mM). [e]Diluted in toluene (MMA/toluene = 1/1 in weight ratio).

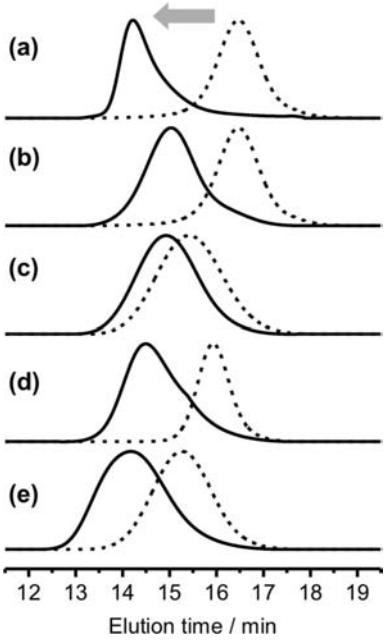

Figure 9. GPC chromatograms before (dashed lines) and after (solid lines) the block copolymerization in Table 5. Entries 1–5 in Table 5 correspond to (a)–(e) in the figure, respectively.

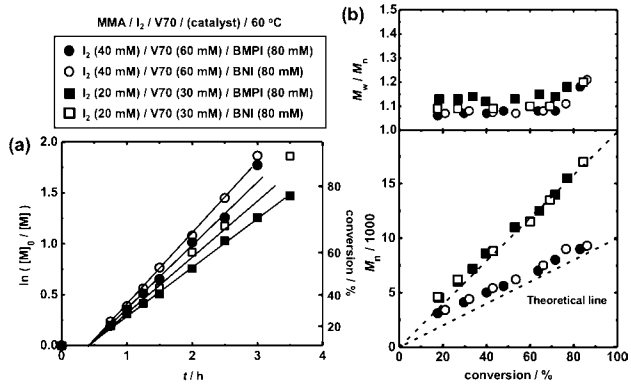

Figure 10. Plots of (a) $\ln([M]_0/[M])$ vs t and (b) M_n and M_w/M_n vs conversion for the MMA/I_2/V70/catalyst systems (in bulk) (60 °C): $[MMA]_0$ = 8 M; $[I_2]_0$ = 40 or 20 mM; $[V70]_0$ = 60 or 30 mM; $[catalyst]_0$ = 80 mM. The catalysts, concentrations of I_2 and V70, and symbols are indicated in the figure.

R-I upon storage. We therefore adapted the I_2/azo method to organic salts.

Figure 10 (filled circles) and Table 6 (entry 1) show the polymerization of MMA (8 M) with I_2 (40 mM), V70 (60 mM), and BMPI (80 mM) at 60 °C. V70 affords alkyl radical R•, and R• reacts with I_2 to yield R-I. Virtually no polymerization occurred at 0.5 h, during which time R• had predominantly reacted with I_2 (rather than monomer), and R-I had accumulated. Because the efficiency of V70 to produce free R• is approximately 0.6–0.7, 60 mM of V70 (in this study) can yield about 80 mM of free R• and hence about 80 mM (theoretical amount) of R-I. After this period, the polymerization smoothly proceeded (Figure 10a). The M_n almost agreed with $M_{n,theo}$, and PDI remained small (about 1.1) throughout the polymerization (Figure 10b).

This method was effective for BMPI, BNI, and higher targeted DPs (200, 400, 800, and 1600) (Figure 10 and Table 6 (entries 2–14)). The addition of tributylamine (TBA) to increase R_p also worked well in this method (Table 6 (entries 8, 10, 12, and 14)). As with MMA, the polymerization of BA was controlled (Table 6 (entry 15)). This method is simple to execute and may practically be useful.

Styrene, Acrylonitrile, and Functional Monomers. Table 7 shows the polymerizations of several monomers: styrene (St) (entry 1), acrylonitrile (AN) (entry 2), and methacrylates functionalized with butyl (BMA), benzyl (BzMA), epoxide (GMA), poly(ethyleneglycol) (PEGMA), hydroxyl (HEMA), and dimethylamino (DMAEMA) groups (entries 3–8). A random copolymerization of MMA and BA was also examined (entry 9). In all of the studied cases, the polymerization was regulated through high conversions (>70%). These results unambiguously demonstrate the great monomer versatility of this system.

Mechanisms. Although the exact mechanism for the reversible activation with the organic salt catalysts remains unclear at the moment, we suppose the following scheme. An iodide anion (A^+I^-) activates Polymer-I, thereby generating Polymer• and an I_2 radical anion ($A^+I_2^{\bullet-}$) (Scheme 3a).

dx.doi.org/10.1021/ja4036016 | J. Am. Chem. Soc. 2013, 135, 11131–11139

Table 6. Polymerizations of MMA and BA with Alkyl Iodide In Situ Formed

entry	monomer	target DP	catalyst	$[monomer]_0/[I_2]_0/[V70]_0/[catalyst]_0$ (mM)	additive	solvent	T (°C)	t (h)	conv (%)	M_n ($M_{n,theo}$)	PDI
1	MMA	100	BMPI	8000/40/60/80		bulk	60	3	86	9300 (8600)	1.21
2	MMA	100	BNI	8000/40/60/80		bulk	60	3	83	9000 (8300)	1.18
3	MMA	200	BMPI	8000/20/30/80		bulk	60	3.5	77	15000 (15000)	1.18
4	MMA	200	BNI	8000/20/30/80		bulk	60	3.5	84	17000 (17000)	1.20
5	MMA	400	BMPI	8000/10/15/80		bulk	60	6	80	30000 (32000)	1.19
6	MMA	400	BNI	8000/10/15/80		bulk	60	6	72	27000 (29000)	1.17
7	MMA	800	BMPI	8000/5/7.5/80		toluene[a]	60	24	70	49000 (56000)	1.25
8	MMA	800	BMPI	8000/5/7.5/80	TBA[b]	toluene[a]	60	24	77	68000 (62000)	1.41
9	MMA	800	BNI	8000/5/7.5/80		toluene[a]	60	24	61	41000 (48000)	1.24
10	MMA	800	BNI	8000/5/7.5/80	TBA[b]	toluene[a]	60	24	72	58000 (58000)	1.44
11	MMA	1600	BMPI	8000/2.5/3.75/80		toluene[a]	60	48	57	88000 (91000)	1.29
12	MMA	1600	BMPI	8000/2.5/3.75/80	TBA[b]	toluene[a]	60	24	58	88000 (93000)	1.33
13	MMA	1600	BNI	8000/2.5/3.75/80		toluene[a]	60	48	57	79000 (91000)	1.23
14	MMA	1600	BNI	8000/2.5/3.75/80	TBA[b]	toluene[a]	60	24	53	90000 (85000)	1.39
15	BA	100	BNI	8000/40/55[c]/320		bulk	110	24	83	13000[d] (11000)	1.30[d]

[a]Diluted in 25 wt % toluene (solution polymerization). [b]$[TBA]_0$ = 40 mM (entries 8, 10, 12, and 14). [c]V65 instead of V70. [d]Determined by GPC with a MALLS detector.

Table 7. Polymerizations of Several Monomers

entry	monomer	target DP	catalyst	$[monomer]_0/[I_2]_0/[V70]_0/[catalyst]_0$ (mM)	solvent	T (°C)	t (h)	conv (%)	M_n[a] ($M_{n,theo}$)	PDI[a]
1	St	100	BNI	8000/40/80[b]/20	bulk	80	10	90	8100 (9300)	1.32
2	AN	200	BNI	8000/20/25/80	EC[c]	75	10	77	14000 (8200)	1.20
3	BMA	200	BNI	8000/20/35/80	bulk	60	5	90	24000 (25000)	1.16
4	BzMA	200	BNI	8000/20/35/80	bulk	60	3	73	27000 (26000)	1.25
5	GMA	200	BNI	8000/20/30/80	bulk	60	3	89	25000 (25000)	1.20
6	PEGMA[d]	200	BNI	8000/20/40/80	bulk	60	5	92	32000 (55000)	1.34
7	HEMA	200	BNI	8000/20/50/80	bulk	60	3	73	28000 (19000)	1.36
8	DMAEMA	200	BNI	8000/20/30/80	bulk	60	3	87	26000 (27000)	1.35
9	BA/MMA	100	BNI	(4000/4000)/40/55[b]/320	bulk	110	24	75	12000 (8500)	1.37

[a]Determined by GPC with a MALLS detector for entries 2–8 and PMMA-calibration for entry 9. [b]AIBN instead of V70. [c]Diluted in 50 wt % ethylene carbonate (EC) (solution polymerization). [d]Molecular weight of monomer = 300.

Scheme 3. Possible Mechanism of Reversible Activation with Organic Salt Catalyst

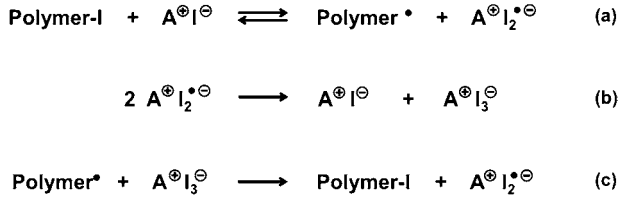

Because $A^+I_2^{\bullet-}$ is not a stable radical, two $A^+I_2^{\bullet-}$ species react with each other to produce A^+I^- and an I_3 anion ($A^+I_3^-$) as stable species (Scheme 3b).[21] The A^+I^- behaves as an activator, whereas $A^+I_3^-$ behaves as a deactivator (Scheme 3c). Polymer$^\bullet$ can thus be deactivated by either $A^+I_2^{\bullet-}$ (Scheme 3a) or $A^+I_3^-$ (Scheme 3c).

We experimentally investigated our supposed mechanism using the MMA polymerization. To probe the formation of $A^+I_3^-$, we measured UV–vis absorption during the polymerization of MMA with CP-I (80 mM) and BNI (40 mM) at 80 °C. Figure 11a shows the spectra at time zero (dotted line) and at 2 h (solid line). At 2 h, a new peak appeared at 360 nm and matched that of pure, independently obtained $A^+I_3^-$ (dashed line). These data prove the formation of $A^+I_3^-$. To confirm that $A^+I_3^-$ acts as a deactivator, we performed a model experiment. We heated a toluene-d_8 solution of Bu_4NI_3 (20 mM) and an azo radical source V601 (40 mM) that produces a model unimer radical of MMA at 60 °C. Figure 11b shows the ^{1}H NMR spectra at time zero and at 1 h. At 1 h, the adduct of the unimer radical and iodine (MMA-I) was observed, which

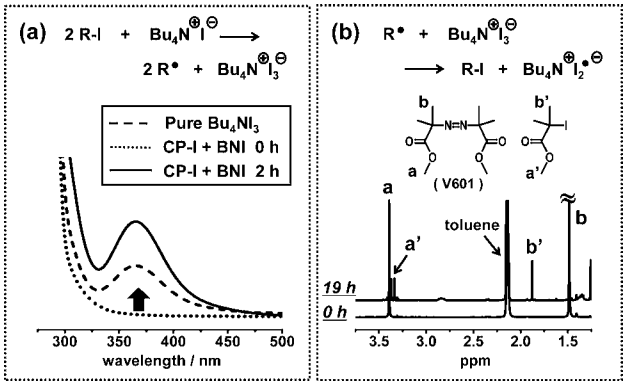

Figure 11. (a) UV spectra of the MMA/CP-I/BNI system (in bulk) (80 °C): $[MMA]_0$ = 8 M; $[CP\text{-}I]_0$ = 80 mM; $[BNI]_0$ = 40 mM at time zero (dotted line) and 2 h (solid line). The broken line shows the spectrum of Bu_4NI_3 (0.02 mM) in MMA. (b) ^{1}H NMR spectra (in the range of 1.25–3.75 ppm) of the toluene-d_8 solution of V601 (40 mM) and Bu_4NI_3 (20 mM) heated at 60 °C for 0 and 19 h. The structure of V601 is shown in the figure.

dx.doi.org/10.1021/ja4036016 | J. Am. Chem. Soc. 2013, 135, 11131–11139

demonstrates that Bu_4NI_3 acts as a deactivator. Thus, the two experiments support the supposed scheme (Scheme 3).

The activation process (Scheme 3a) may occur in two ways. In one way, it can occur thorough an iodine-bridged transition state (Scheme 4a) as in ATRP (inner sphere electron transfer).[13] In the other way, it can occur via single electron transfer (SET) forming a donor radical ($A^+I^•$) and an acceptor anion (Polymer-I^-) as kinetically important intermediates (Scheme 4b) as in SET-LRP (outer sphere electron transfer).[22] The contributions of the two mechanisms in the present system are not clear at the moment.

Scheme 4. Possible Mechanisms of Reversible Activation via (a) Iodine-Bridged Transition State and (b) SET

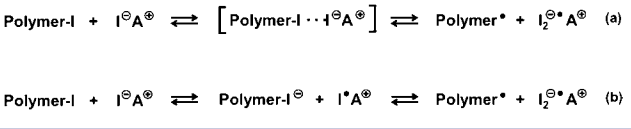

In organic chemistry, organic amines and iodine anion are well recognized as outer sphere electron donors to induce SET particularly in polar solvents.[7c,21] They have been employed for irreversible reactions.

The use of organic electron donor $SO_2^{•-}$ is also precedent in polymer chemistry. SET-DTLPR[23] uses SET from $SO_2^{•-}$ (donor) to iodoform (acceptor) to initiate polymerization (as irreversible reaction), and the polymerization is then controlled by DT.

Activation Rate Constant. The pseudofirst-order activation rate constant k_{act} (Scheme 1a), which represents the frequency of the activation−deactivation cycle, is a fundamental parameter for determining the polydispersity.[16] We experimentally determined the k_{act} of PMMA-I (M_n = 5500 and PDI = 1.19) in the polymerizations of MMA by varying the concentrations of the catalysts BMPI and BNI. The method for determining k_{act} was a previously reported gel permeation chromatography (GPC) peak resolution method (Supporting Information).[24] We focused on the polymer dormant species PMMA-I, i.e., the k_{act} in the polymer region. According to Schemes 1a and 1c, k_{act} takes the form

$$k_{act} = k_a[A^+I^-] \quad (1)$$

Figure 12 shows the plot of k_{act} vs $[catalyst]_0$ at 90 °C. For both BMPI (circle) and BNI (square), the plot was linear, as expected from eq 1. The slope of the line gives k_a to be 0.30 M^{-1} s^{-1} for BMPI and 0.43 M^{-1} s^{-1} for BNI. (The system also includes DT.[14,16] However, the rate constant of DT is so small[8] that the contribution of DT to k_{act} is negligible.) Importantly, the k_a values for BMPI and BNI are larger than the k_a value (0.13 M^{-1} s^{-1}) for tetramethylethylenediamine (TMEDA) (triangle),[8] which is a representative good amine catalyst we previously studied. These larger k_a values clearly illustrate the high reactivity of the organic salts and explain why they were effective even at mild temperatures. In addition, the k_a values for BMPI and BNI are similar to that (0.45 M^{-1} s^{-1}) in a representative ATRP of St with PSt-Br and CuBr/dHbipy catalyst at 110 °C,[25] where PSt is polystyrene and dHbipy is 4,4′-di-*n*-heptyl-2,2′-bipyridine. Because the monomer, halogen, and temperature are different between our systems and that ATRP, this information does not directly compare the activity of the three catalysts; nonetheless, it still clearly suggests that our systems are virtually as effective as this good ATRP system.

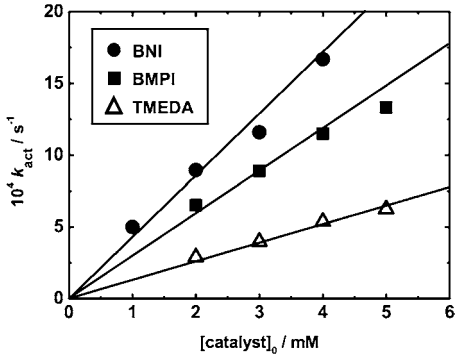

Figure 12. Plot of k_{act} vs $[catalyst]_0$ for the MMA/PMMA-I/catalyst systems (90 °C). The catalysts and symbols are indicated in the figure.

CONCLUSIONS

R-I reacted with organic salts to reversibly generate R•. With this new reaction, the organic salts were successfully employed as powerful and pervasive catalysts for RCMP. The catalysts enabled the synthesis of high-molecular-weight polymers (up to M_n = 140 000) and the control of acrylate polymerization. The catalysts exhibited high monomer versatility. Methacrylate and acrylate block copolymers were also synthesized without restriction on the monomer order of addition. The I_2/azo method was effective and offered a simplified synthetic procedure. The k_a values were experimentally determined for BNI and BMPI, and the results quantitatively demonstrate their high reactivity. The described catalyst system used only inexpensive compounds and was free from metals. The facile operation and access to a large variety of polymer designs may be greatly beneficial in a variety of applications.

ASSOCIATED CONTENT

Supporting Information

Experimental information, preparation of CP-TEMPO, and determination of k_{act}. This material is available free of charge via the Internet at http://pubs.acs.org.

AUTHOR INFORMATION

Corresponding Author

agoto@scl.kyoto-u.ac.jp; kaji@scl.kyoto-u.ac.jp

Notes

The authors declare no competing financial interest.

ACKNOWLEDGMENTS

This work was supported by Grants-in-Aid for Scientific Research from the Japan Society of the Promotion of Science (JSPS) and the Japan Science and Technology Agency (JST). A high-resolution 800 MHz ^{1}H NMR experiment (Figure 5) was carried out with the NMR spectrometer in the Joint Usage/Research Center (JURC) at Institute for Chemical Research, Kyoto University.

REFERENCES

(1) (a) Hegedus, L. S. *J. Am. Chem. Soc.* **2009**, *131*, 17995−17997. (b) Kiesewetter, M. K.; Shin, E. J.; Hedrick, J. L.; Waymouth, R. M. *Macromolecules* **2010**, *43*, 2093−2107. (c) Mukherjee, S.; Yang, J. W.; Hoffmann, S.; List, B. *Chem. Rev.* **2007**, *107*, 5471−5569. (d) Biju, A. T.; Kuhl, N.; Glorius, F. *Acc. Chem. Res.* **2011**, *44*, 1182−1195. (e) Kano, T.; Shirozu, F.; Akakura, M.; Maruoka, K. *J. Am. Chem. Soc.* **2012**, *134*, 16068−16073. (f) Kakuchi, R.; Chiba, K.; Fuchise, K.;

Sakai, R.; Satoh, T.; Kakuchi, T. *Macromolecules* **2009**, *42*, 8747−8750. (g) Raynaud, J.; Gnanou, Y.; Taton, D. *Macromolecules* **2009**, *42*, 5996−6005.
(2) (a) Neumann, W. P. *Synthesis* **1987**, 665−683. (b) Chatgilialoglu, C.; Newcomb, M. *Adv. Organomet. Chem.* **1999**, *44*, 67−112. (c) Studer, A.; Amrein, S. *Synthesis* **2002**, 835−849.
(3) Goto, A.; Zushi, H.; Hirai, N.; Wakada, T.; Tsujii, Y.; Fukuda, T. *J. Am. Chem. Soc.* **2007**, *129*, 13347−13354.
(4) (a) Goto, A.; Hirai, N.; Wakada, T.; Nagasawa, K.; Tsujii, Y.; Fukuda, T. *Macromolecules* **2008**, *41*, 6261−6264. (b) Goto, A.; Tsujii, Y.; Fukuda, T. *Polymer* **2008**, *49*, 5177−5185. (c) Goto, A.; Nagasawa, K.; Shinjo, A.; Tsujii, Y.; Fukuda, T. *Aust. J. Chem.* **2009**, *62*, 1492−1495. (d) Goto, A.; Hirai, N.; Nagasawa, K.; Tsujii, Y.; Fukuda, T.; Kaji, H. *Macromolecules* **2010**, *43*, 7971−7978.
(5) (a) Vana, P.; Goto, A. *Macromol. Theory Simul.* **2010**, *19*, 24−35. (b) Yorizane, M.; Nagasuga, T.; Kitayama, Y.; Tanaka, A.; Minami, H.; Goto, A.; Fukuda, T.; Okubo, M. *Macromolecules* **2010**, *43*, 8703−8705. (c) Kuroda, T.; Tanaka, A.; Taniyama, T.; Minami, H.; Goto, A.; Fukuda, T.; Okubo, M. *Polymer* **2012**, *53*, 1212−1218.
(6) Goto, A.; Tsujii, Y.; Kaji, H. In *Fundamentals of Controlled/Living Radical Polymerization*; Tsarevsky, N. V., Sumerlin, B. S., Eds.; Royal Society of Chemistry: UK, 2013; pp 250−286.
(7) (a) Stevenson, D. P.; Coppinger, G. M. *J. Am. Chem. Soc.* **1962**, *84*, 149−152. (b) Lautenberger, W. J.; Jones, E. N.; Miller, J. G. *J. Am. Chem. Soc.* **1968**, *90*, 1110−1115. (c) Ishibashi, H.; Haruki, S.; Uchiyama, M.; Tamura, O.; Matsuo, J. *Tetrahedron Lett.* **2006**, *47*, 6263−6266.
(8) Goto, A.; Suzuki, T.; Ohfuji, H.; Tanishima, M.; Fukuda, T.; Tsujii, Y.; Kaji, H. *Macromolecules* **2011**, *44*, 8709−8715.
(9) Goto, A.; Tsujii, Y.; Kaji, H. *ACS Symp. Ser.* **2012**, *1100*, 305−315.
(10) Ohtsuki, A.; Goto, A.; Kaji, H. *Macromolecules* **2013**, *46*, 96−102.
(11) For reviews on LRP: (a) Tsarevsky, N. V.; Sumerlin, B. S. *Fundamentals of Controlled/Living Radical Polymerization*; Royal Society of Chemistry: UK, 2013. (b) Matyjaszewski, K.; Möller, M. *Polymer Science: A Comprehensive Reference*; Elsevier: Amsterdam, 2012. (c) Braunecker, W. A.; Matyjaszewski, K. *Prog. Polym. Sci.* **2007**, *32*, 93−146. (d) Moad, G.; Solomon, D. H. *The Chemistry of Radical Polymerization*; Elsevier: Amsterdam, 2006.
(12) For reviews on nitroxide, dithioester, and telluride LRPs: (a) Sciannamea, V.; Jérôme, R.; Detrembleur, C. *Chem. Rev.* **2008**, *108*, 1104−1126. (b) Moad, G.; Rizzardo, E.; Thang, S. H. *Aust. J. Chem.* **2009**, *62*, 1402−1472. (c) Keddie, D. J.; Moad, G.; Rizzado, E.; Thang, S. H. *Macromolecules* **2012**, *45*, 5321−5342. (d) Yamago, S. *Chem. Rev.* **2009**, *109*, 5051−5068.
(13) For ATRP: (a) Wang, J. S.; Matyjaszewski, K. *J. Am. Chem. Soc.* **1995**, *117*, 5614−5615. (b) Kato, M.; Kamigaito, M.; Sawamoto, M.; Higashimura, T. *Macromolecules* **1995**, *28*, 1721−1723. (c) Ouchi, M.; Terashima, T.; Sawamoto, M. *Chem. Rev.* **2009**, *109*, 4963−5050. (d) Lena, F.; Matyjaszewski, K. *Prog. Polym. Sci.* **2010**, *35*, 959−1021. (e) Matyjaszewski, K. *Macromolecules* **2012**, *45*, 4015−4039.
(14) For a review on iodide-mediated LRP: David, G.; Boyer, C.; Tonnar, J.; Ameduri, B.; Lacroix-Desmazes, P.; Boutevin, B. *Chem. Rev.* **2006**, *106*, 3936−3962.
(15) (a) Zetterlund, P. B.; Kagawa, Y.; Okubo, M. *Chem. Rev.* **2008**, *108*, 3747−3794. (b) Rosen, B. M.; Percec, V. *Chem. Rev.* **2009**, *109*, 5069−5119. (c) Satoh, K.; Kamigaito, M. *Chem. Rev.* **2009**, *109*, 5120−5156. (d) Boyer, C.; Bulmus, V.; Davis, T. P.; Ladmiral, V.; Liu, J.; Perrier, S. *Chem. Rev.* **2009**, *109*, 5402−5436. (e) Monteiro, M. J.; Cunningham, M. F. *Macromolecules* **2012**, *45*, 4939−4957. (f) Monteiro, M. J.; Cunningham, M. F. *Macromolecules* **2012**, *45*, 4939−4957. (g) Yamago, S.; Nakamura, Y. *Polymer* **2013**, *54*, 981−994.
(16) For reviews on kinetics of LRP: (a) Fukuda, T. *J. Polym. Sci., Part A: Polym. Chem.* **2004**, *42*, 4743−4755. (b) Fischer, H. *Chem. Rev.* **2001**, *101*, 3581−3618. (c) Goto, A.; Fukuda, T. *Prog. Polym. Sci.* **2004**, *29*, 329−385. (d) Fukuda, T.; Goto, A. In *Polymer Science: A Comprehensive Reference*; Matyjaszewski, K., Möller, M., Eds.; Elsevier: Amsterdam, 2012; pp 120−157.
(17) (a) Moad, G.; Rizzardo, E. *Macromolecules* **1995**, *28*, 8722−8728. (b) Goto, A.; Fukuda, T. *Macromol. Rapid Commun.* **1999**, *20*, 633−636. (c) Schulte, T.; Studer, A. *Macromolecules* **2003**, *36*, 3078−3084.
(18) Ando, T.; Kamingaito, M.; Sawamoto, M. *Macromolecules* **1997**, *30*, 4507−4510.
(19) Chong, Y. K.; Le, T. P. T.; Moad, G.; Rizzardo, E.; Thang, S. H. *Macromolecules* **1999**, *32*, 2071−2074.
(20) (a) Lacroix-Desmazes, P.; Severac, R.; Boutevin, B. *Macromolecules* **2005**, *38*, 6299−6309. (b) Tonnar, J.; Lacroix-Desmazes, P. *Angew. Chem., Int. Ed.* **2008**, *47*, 1294−1297.
(21) Gardner, J. M.; Abrahamsson, M.; Farnum, B. H.; Meyer, G. J. *J. Am. Chem. Soc.* **2009**, *131*, 16206−16214.
(22) Percec, V.; Guliashvili, T.; Ladislaw, J. S.; Wistrand, A.; Stjerndahl, A.; Sienkowska, M. J.; Monteiro, M. J.; Sahoo, S. *J. Am. Chem. Soc.* **2006**, *128*, 14156−14165.
(23) Percec, V.; Popov, A. V.; Ramirez-Castillo, E.; Coelho, J. F. J.; Hinojosa-Falcon, L. A. *J. Polym. Sci., Part A: Polym. Chem.* **2004**, *42*, 6267−6282.
(24) Goto, A.; Terauchi, T.; Fukuda, T.; Miyamoto, T. *Macromol. Rapid Commun.* **1997**, *18*, 673−681.
(25) Ohno, K.; Goto, A.; Fukuda, T.; Xia, J.; Matyjaszewski, K. *Macromolecules* **1998**, *31*, 2699−701.